



Estimation of fracture half-length with fast Gaussian pressure transient and RTA methods: Wolfcamp shale formation case study

Ahmed Farid Ibrahim^{1,2} · Ruud Weijermars^{1,2}

Received: 8 May 2023 / Accepted: 19 August 2023 / Published online: 12 September 2023
© The Author(s) 2023

Abstract

Accurate estimation of fracture half-lengths in shale gas and oil reservoirs is critical for optimizing stimulation design, evaluating production potential, monitoring reservoir performance, and making informed economic decisions. Assessing the dimensions of hydraulic fractures and the quality of well completions in shale gas and oil reservoirs typically involves techniques such as chemical tracers, microseismic fiber optics, and production logs, which can be time-consuming and costly. This study demonstrates an alternative approach to estimate fracture half-lengths using the Gaussian pressure transient (GPT) Method, which has recently emerged as a novel technique for quantifying pressure depletion around single wells, multiple wells, and hydraulic fractures. The GPT method is compared to the well-established rate transient analysis (RTA) method to evaluate its effectiveness in estimating fracture parameters. The study used production data from 11 wells at the hydraulic fracture test site 1 in the Midland Basin of West Texas from Upper and Middle Wolfcamp (WC) formations. The data included flow rates and pressure readings, and the fracture half-lengths of the 11 wells were individually estimated by matching the production data to historical records. The GPT method can calculate the fracture half-length from daily production data, given a certain formation permeability. Independently, the traditional RTA method was applied to separately estimate the fracture half-length. The results of the two methods (GPT and RTA) are within an acceptable, small error margin for all 5 of the Middle WC wells studied, and for 5 of the 6 Upper WC wells. The slight deviation in the case of the Upper WC well is due to the different production control and a longer time for the well to reach constant bottomhole pressure. The estimated stimulated surface area for the Middle and Upper WC wells was correlated to the injected proppant volume and the total fluid production. Applying RTA and GPT methods to the historic production data improves the fracture diagnostics accuracy by reducing the uncertainty in the estimation of fracture dimensions, for given formation permeability values of the stimulated rock volume.

Keywords Fracture half-length · Formation permeability · Gaussian pressure transient · Rate transient analysis

Abbreviations

EUR	Estimated ultimate recovery
GOR	Gas oil ratio
GPT	Gaussian pressure transient
HFTS-1	Hydraulic fracture test site 1
MWC	Middle Wolfcamp

RTA	Rate transient analysis
UWC	Upper Wolfcamp
WC	Wolfcamp

Physical parameters

A_c	Total fracture surface area, ft ²
B_o	Formation volume factor, bbl/stb
c_t	Total compressibility, psi ⁻¹
D_h	Hydraulic diffusivity
h	Pay-zone height, ft
h_f	Fracture height, ft
k	Formation permeability, nD
n_f	Total number of fractures
P_0	Initial reservoir pressure
P_{BH}	Bottomhole pressure, psi
$P(r, t)$	Radial pressure transient, psi
$q_w(t)$	Observed well rate,

✉ Ahmed Farid Ibrahim
ahmed.ibrahim@kfupm.edu.sa

¹ Department of Petroleum Engineering, College of Petroleum Engineering and Geosciences (CPG), King Fahd University of Petroleum & Minerals, KFUPM, 31261 Dhahran, Saudi Arabia

² Center for Integrative Petroleum Research (CIPR), College of Petroleum Engineering and Geosciences (CPG), King Fahd University of Petroleum & Minerals, KFUPM, 31261 Dhahran, Saudi Arabia

r_w	Well radius, ft
R_{sob}	Solution gas oil ratio, scf/stb
T	Temperature, R
x_f	Fracture half length, ft
φ	Formation porosity
μ	Fluid viscosity

Introduction

Hydraulic fracturing is used to enhance the production of hydrocarbons from tight and unconventional oil and gas reservoirs by creating highly conductive fractures that connect the wellbore to the formation (Holditch 2010; Peebles et al. 2018; Al-Fatlawi et al. 2019a, b; Fujian et al. 2019; King 2012; Smith and Montgomery 2015; Ibrahim et al. 2018). Geomechanical characterization of shale can be used to estimate the mechanical properties and behavior of shale formations at a small scale. This characterization is important for understanding the response of shales to mechanical loading, such as stress–strain behavior, elastic and plastic deformation, fracture propagation, and rock strength (Li and Sakhaee-Pour 2016; Sakhaee-Pour and Li 2019; Esatyana et al. 2020). Although hydraulic fracturing appears to be a straightforward process, it poses numerous challenges and complications due to uncertainties surrounding reservoir characteristics, fracture growth patterns, and fluid and proppant placement, which could jeopardize the effectiveness of each fracture treatment (Cipolla et al. 2010). In addition, a better understanding of the fluid transport properties of the shale matrix plays a vital role in improving hydrocarbon recovery by optimizing hydraulic fracturing, identifying sweet spots, predicting fluid behavior, enhancing stimulation design, and improving wellbore management (Alipour et al. 2021, 2022, ; Sakhaee-Pour and Bryant 2012; Tran and Sakhaee-Pour 2017, 2018a, b, 2019).

Following treatment, a variety of techniques can be used to constrain the fracture dimensions, growth behavior, and fracture interactions with the surrounding reservoir (Barree et al. 2002). Based on the information obtained from diagnostic tests, iterative economic assessments are performed to establish the optimal treatment plan (Warpinski, 2009). Enhancing fracture diagnostic techniques is crucial for fracture stimulation treatment design, execution, and monitoring (Maxwell et al. 2010). Among the techniques used to evaluate the fracture operations are chemical tracers, which may identify the individual production contribution of specific fracture stages, as well as reveal the existence of any communication with adjacent fractured wells (Tian et al. 2016a, b). However, these techniques are inaccurate, and tracer tests remain expensive, which precludes their routine use.

Real-time microseismic monitoring (Murillo et al. 2014) and fiber optics (Pakhotina et al. 2020; Sakaida et al. 2022) also are increasingly used to constrain the fracture geometry,

but cost control lead companies to reserve microseismic, fiber, and tiltmeter studies typically for a limited number of wells. Most diagnostic methods are syn-fracture and post-fracture, requiring the insertion of additional tools or injection of chemicals into the wells.

There is growing interest in the oil industry to use production data to better understand the hydraulic fracture systems of wells after they have been stimulated. Two widely used methods for diagnosing fractures and estimating formation and fracture parameters without incurring additional costs are rate transient analysis (RTA) and pressure transient analysis (PTA). RTA is a well-established technique in petroleum engineering and is commonly used to predict future production behavior by characterizing fracture and reservoir parameters (El-Banbi and Wattenbarger 1998; Ibrahim et al. 2020; Ibrahim and Wattenbarger 2006; Clarkson 2013; Nguyen et al. 2020; Shabaniet al. 2022).

Various RTA methods can be used, such as straight-line analysis, history-matching, and type-curve analysis, in addition to hybrid methods. Straight-line analysis determines the reservoir and fracture parameters by analyzing production data using specialized plots. These plots linearize the production data with respect to specific flow regimes that are similar to PTA (Lee et al. 2003; Shabaniet al. 2022). Various diagnostic plots can be analyzed to identify the different flow regimes caused by the hydraulic fracture geometry and reservoir properties. In the linear flow regime, pressure decline over time is proportional to the square root of time, which is mainly influenced by the stimulated area and formation permeability. The RTA technique was first introduced by Wattenbarger et al. (1998) to examine production data from vertically fractured wells. They assumed a rectangular homogeneous reservoir and an infinitely conductive hydraulic fracture. From the square root of time plots, they determined the values of the drainage area and permeability. Researchers have since advanced this work by accounting for the nonlinear behavior of gas properties (Ibrahim and Wattenbarger, 2006), gas slippage, and adsorption effects (Nobakht et al. 2012). The traditional RTA straight line approach will be discussed in Sect. "Rate transient analysis".

The main limitations of RTA methods are related to the assumption of RTA that the flow behavior remains constant over time for a certain flow regime. In addition, RTA is typically based on simple flow mechanisms such as linear flow, radial flow, bilinear flow, spherical flow, and pseudo-steady state flow. Complex flow mechanisms such as fracture-matrix interaction, and multi-phase flow can be difficult to model and may limit the accuracy of the analysis.

Recently, a new solution was obtained for the pressure transient related to well interventions by assuming a constant bottom hole pressure (Weijermars 2021, 2022a, b). The solution involves a Gaussian probability density

function and has therefore been coined as the Gaussian pressure-transient (GPT) solution (Weijermars 2021). Based on the new solution of the pressure diffusion equation, a Gaussian PTA method (see Sect. "Gaussian pressure transient analysis") can be formulated to estimate fracture half-lengths, after first having obtained a suitable value for the hydraulic diffusivity based on history matching production data with a Gaussian decline curve analysis method (Weijermars and Afagwu 2022).

The Wolfcamp Shale Formation is a prominent geological formation known for its vast reserves of oil and gas. Located primarily in the Permian Basin in Texas, it has gained significant attention as a major target for energy exploration and production. The hydraulic fracturing process in the Wolfcamp Shale involves multiple stages, where each stage is typically associated with a specific zone along the wellbore. Horizontal drilling techniques are employed to access a larger surface area of the shale formation, maximizing the potential for hydrocarbon recovery.

The HFTS-1 (hydraulic fracturing test site 1) is a field-based research program focused on hydraulic fracturing. It is situated in the eastern region of the Midland Basin, between the Central Basin Platform and the Eastern Shelf. The program aims to address fundamental questions regarding hydraulic fracture behavior in unconventional resource development. Collaboration among industry experts, academia, and government is fostered to acquire valuable datasets. The test wells are located in Reagan County, Texas, which is covered by a high-quality 3-D seismic survey, and surrounded by both horizontal and vertical producing wells. As part of study, a total of 11 horizontal wells were drilled in the Upper and Middle Wolfcamp formations, with five wells in the Middle Wolfcamp and six in the Upper Wolfcamp (Ciezobka et al. 2018).

The present study estimates the fracture half-length of Wolfcamp (WC) study wells using the Gaussian pressure transient (GPT) method and the traditional rate transient analysis (RTA) method and compares the results, in order to establish the practical value of the GPT method.

Methodology

This section briefly explains the traditional RTA (Sect. "Rate transient analysis") and GPT method (Sect. "Gaussian pressure transient analysis") methodologies to determine the fracture-half-lengths of the selected study wells from each method independently and the results were compared in Sect. "Discussion".

Rate transient analysis

RTA relies on the pressure diffusivity equation in a rectangular reservoir with a closed outer boundary (reflecting no-flow boundary conditions), while the inner boundary at the wellbore the well was assumed to be producing at constant flowrate as shown in Fig. 1a, b. The change of the dimensionless pressure over dimensionless time is given by:

$$P_{WD} = \frac{\pi}{2} \left(\frac{y_e}{x_f} \right) \left[\frac{1}{3} + \left(\frac{x_f}{y_e} \right)^2 t_{Dxf} \right] - \frac{2}{\pi^2} \left(\frac{y_e}{x_f} \right) \sum_{n=1}^{\infty} \frac{1}{n^2} \exp \left[-n^2 \pi^2 \left(\frac{x_f}{y_e} \right)^2 t_{Dxf} \right] \quad (1)$$

where dimensionless variables are defined by:

$$P_{WD} = \frac{kh(P_0 - P_{BH})}{141.2qB\mu} \quad (2)$$

$$t_{Dxf} = \frac{0.00633kt}{\varphi\mu c_r x_f^2} \quad (3)$$

where q is the observed well rate during flow tests. Ambient parameters are the formation volume factor, B , fluid viscosity, μ , permeability, k , initial reservoir pressure, P_0 , bottom hole pressure, P_{BH} , the pay-zone height, h , the fracture height h_f is assumed to be equal to h , the number of layers in a linear layered reservoir, n , and the well radius, r .

When applying RTA to hydraulically fractured wells, the E1-Banbi and Wattenbarger (1998) solution, which assumes linear flow and infinite fracture conductivity can be used, and the short-term approximation for Eq. (1) simplifies to:

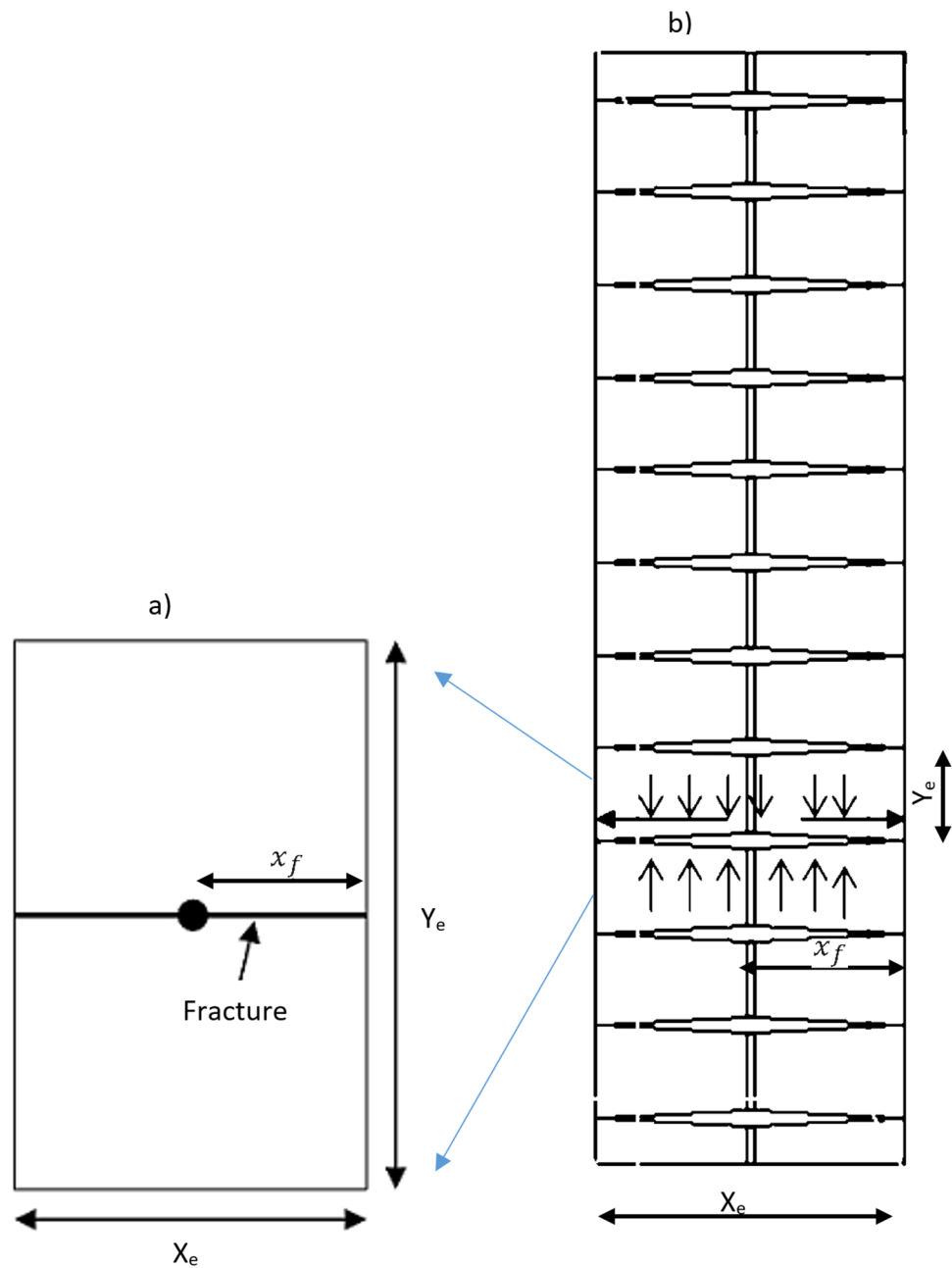
$$P_{WD} = \sqrt{\pi t_{Dxf}} \quad (4)$$

By substituting Eqs. (2) and (3) into Eq. (4), the dimensional form of Eq. (4) becomes:

$$\frac{(P_0 - P_{BH})}{q} = \frac{79.65B\mu}{\sqrt{(\varphi\mu c_r)_i} \sqrt{kA_c}} \sqrt{t} \quad (5)$$

To determine X_f , the straight-line technique can be applied, where diagnostic plots are used to define the flow regimes, and then the linear flow regime is further investigated through the specialized plot to estimate the completion and the formation properties. Figure 2a depicts a diagnostic plot identifying the linear flow regime from its slope of 1/2. Figure 2b is a more specialized and definitive plot for identifying the linear flow behavior (Ibrahim and Wattenbarger 2005; Dheyauldeen et al. 2022). In the Cartesian plot, a straight line with a slope m is identified, from which $\sqrt{kA_c}$ can be calculated (E1-Banbi and Wattenbarger 1998):

Fig. 1 **a** Coordinate system and fracture orientation, in map views, assumed in the traditional RTA approach of Eq. (1), with vertical fracture of half-length x_f extending from the horizontal well in the center of a rectangular reservoir section. **b** The same Eq. (1) solution is used for multi-fractured horizontal wells, where x_f is then represented by n_f fractures with individual fracture half-lengths of $x_f * n_f$



$$\sqrt{k}A_c = \frac{79.65B\mu}{\sqrt{(\varphi\mu c_t)_i}} \left(\frac{1}{m}\right) \quad (6)$$

A_c is the total fracture surface area which account for the the fractures area that effectvely participate in the fluid production and it can be calculated as follows;

$$A_c = 4x_f h_f \text{ for } n_f = 1 \quad (7)$$

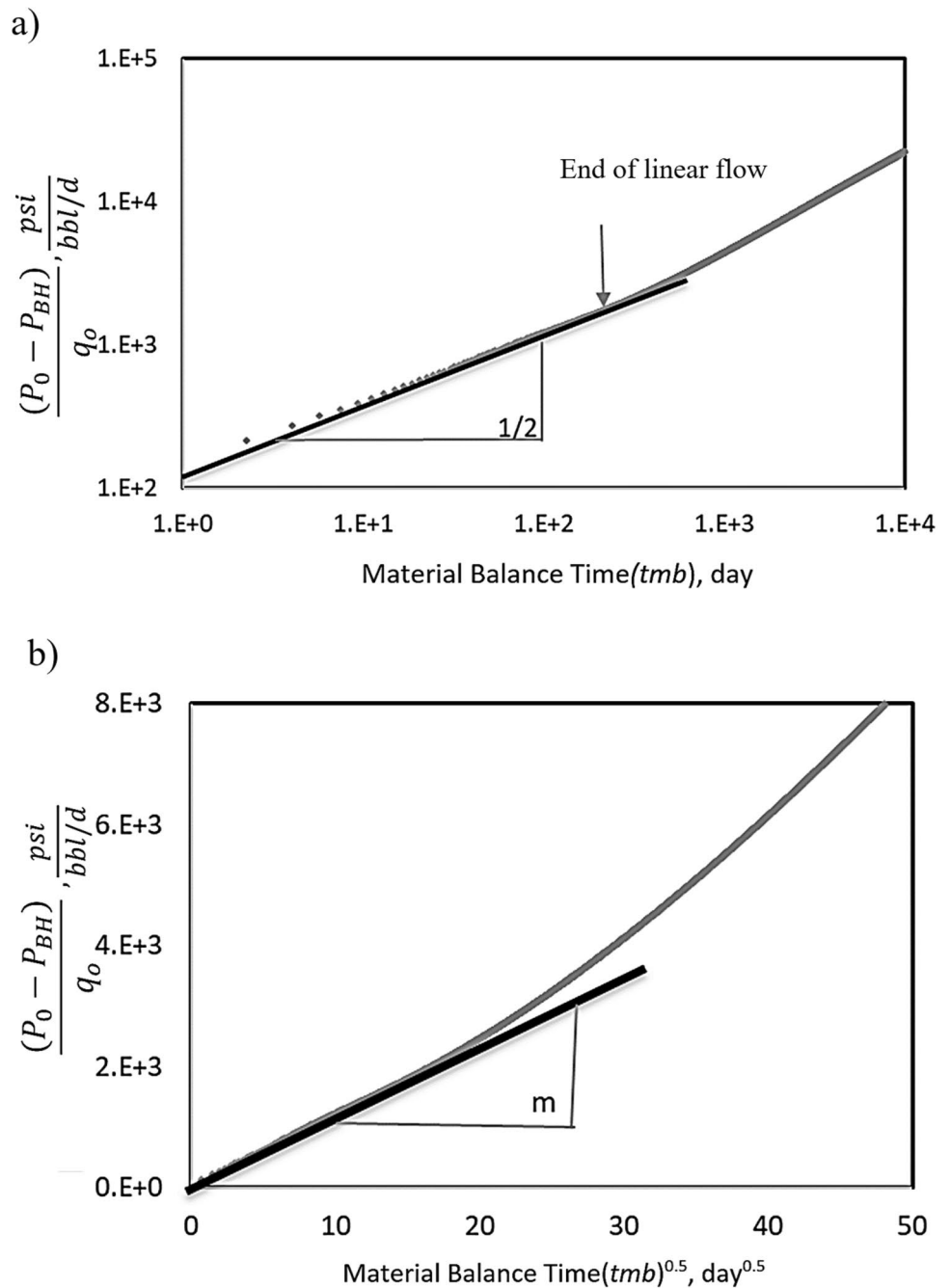
$$A_c = 4x'_f h_f \text{ for } n_f > 1, \text{ and} \quad (8)$$

$$x'_f = x_f * n_f \quad (9)$$

φ, μ, c_t are the formation porosity, fluid viscosity, and total formation compressibility, respectively, and k is the formation permeability.

When applying RTA, the pressure drop ($P_0 - P_{BH}$) imposed via the well system to the reservoir is normalized using the production rate. The normalized pressure difference and material balance time (tmb) are then used in an RTA plot for A_c characterization (Nashawi and

Fig. 2 RTA for a shale well **a** diagnostic plot, and **b** linear flow regime specialized plot



Malallah 2006). The use of log–log diagnostic plots of $(P_0 - P_{BH})/q_o$ and the drop-pressure/oil rate derivative function, $t [\Delta(p)/q_o]'$, are recommended for flow-regime diagnostics. This requires the construction of (1) a diagnostic log–log plot of $(\Delta p)/q_o$ versus t (Fig. 2a), and (2) a log–log plot of $t [\Delta(p)/q_o]'$ versus t (Fig. 2b). The flow regimes can then be determined as a function of the tangent slopes to the plotted data.

Gaussian pressure transient analysis

GPT solutions for fluid flow in porous media assume a constant bottomhole pressure in the well system, which was derived by Weijermars (2021). For a vertical well in radial coordinates, the solution is (Weijermars 2022a):

$$q_w(t) = \frac{(P_0 - P_{BH})}{D_h t} \frac{k}{\mu} \frac{\pi r h}{B} e^{\frac{-r^2}{4D_h t}} \tag{10}$$

P_{BH} is the assumed constant bottomhole pressure in the well. Equation (10) is a drastic departure from the classical well-testing Eq. (1) because, in the new solution of Eq. (10), the well rate is not used (nor needed) to find the pressure advance. Reconciling the well-test Eq. (1) and the new GPT solution of Eq. (10) is not possible: the GPT solution assumes as a constant P_{BH} through the well life, while the well-test Eq. (1) assumes the P_{BH} drops according to $P(r,t)$. However, the GPT solution can solve for the spatial and temporal pressure transient advance everywhere in the reservoir.

For the case of a fractured well, the appropriate solution of the pressure transient is given by the following equation (Weijermars 2022a, b), with the fractures orientated in the x -direction as Fig. 1, rather than in the y -direction as was used in the original study:

$$q_w(t) = 2n_f x_f h_f \frac{k}{\mu B} \frac{P_0 - P_{BH}}{D_h t} y e^{-\left(\frac{y^2}{4D_h t}\right)} \quad (11)$$

We only consider the half-length x_f of the fracture that is effectively propped (as is the case in traditional RTA (Fig. 1a, b), which corresponds to the fracture length where approximately infinite conductivity is achieved. The well rate can then be computed from Eq. (11), considering influx at $y=1$ unit length from the diffusion source for a recommended standard approach (Weijermars 2022a, b).

In case field units are used as inputs, as is commonly the case in the US petroleum industry, one needs to make sure to use Eq. (11) with the following conversion factors:

$$q_w(t) = \frac{C_1 C_2}{C_3} \frac{2n_f x_f h_f k (P_0 - P_{BH})}{\mu B D_h t} y e^{-\frac{y^2}{4D_h t}} \quad (12)$$

The conversion factors have the following values; the use of three, rather than a single consolidated conversion is preferred here, because it is simpler to explain stepwise how the various physical parameters factor into the conversion of units.

$C_1 = 0.178$ bbls/ft³. This factor arises because the input units in ft on the right hand side lead to cubic ft, which needs conversion to oil bbls (for subsequent multiplication with the volume factor in bbl/stb to end up with stb for the left-hand side well rate). The required conversion factor is $1 \text{ ft}^3 = 0.178108$ bbls. If we work with gas wells, the conversion factor $C_1 = 0.001$ Mcf/ft³, because $1 \text{ ft}^3 = 0.001$ Mcf, and the produced gas volume will be expressed in Mcf.

$C_2 = 1.062\text{E-}14$ ft²/mD. This factor is needed to convert square ft units of permeability and prorated for inputs in mD. The required conversion factor is $1 \text{ mD} = 1.062 \times 10^{-14}$ ft².

$C_3 = 1.678\text{E-}12$ psi.d/cPoise. This factor is needed if the viscosity input is in cPoise, then conversion of viscosity to psi.d will result in output for well rate in stb/d. The required conversion factor is: $1 \text{ cPoise} = 1.678 \times 10^{-12}$ psi.d.

The required hydraulic diffusivity for a relevant reservoir section can be obtained by matching historic production data, using the following Gaussian decline curve analysis equation (Weijermars 2022a, b):

$$q_w(t) = q_i \frac{1}{t'} e^{\frac{1}{4D_h t'} \left(1 - \frac{1}{t'}\right)} \quad (13)$$

Equation (10) can be applied using daily production data. For oil wells, the initial well rate q_i for the first day of production is set at 1 bbl/d; for gas well q_i is 1 Mscf/d. The term $\frac{1}{t'} e^{\frac{1}{4D_h t'} \left(1 - \frac{1}{t'}\right)}$ is comprised of non-dimensional parameters, but normalization of its parameters used unit measures (Weijermars 2022a, b), such that substitution of t' in dimensionless units (e.g., $t' = 1$ for $t_{\text{dimensional}} = 1$ day, or $t' = 10$ for $t_{\text{dimensional}} = 10$ days, etc.) and dimensionless D_h' (such that $D_h' = 1$ equals to a dimensional input $D_{h_{\text{dimensional}}}$ of 1 ft²/d) yields physically accurate results.

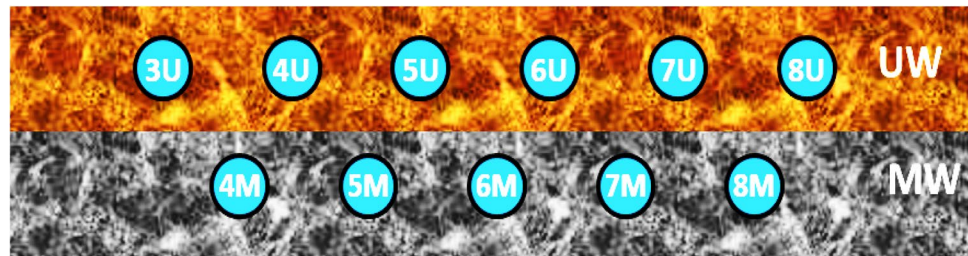
Results

The GPT and RTA techniques were used to analyze production data of eleven shale wells completed during the US Department of Energy (DOE) hydraulic fracture test (HFTS-1) project conducted in the Middle and Upper WC formation (Midland Basin, West Texas). Numerous studies have been conducted using HFTS-1 project data, but the well data were not publicly released until analyzed in non-dimensional plots (Weijermars et al. 2020), and dimensional plots (Tugan and Weijermars 2022) in prior studies, for which permission was obtained from the operator. In the present study, these data are used for the first time to estimate the fracture half-lengths of the wells using two independent methods (RTA and GPT), improving earlier GPT estimations of fracture half-lengths by Weijermars (2022b).

Figure 3 displays a gun barrel view for the wells, with six wells landed in the Upper WC, and 5 wells in the Middle WC. The average stage length used for these wells was 175 ft and the number of stages varied between 37 and 49 stages, as shown in Fig. 4. The number of clusters per stage varied between 3 and 5 clusters/stage (Weijermars et al. 2020). The GPT and RTA techniques were used to estimate the total stimulated area for the whole well based on the production data, then the total number of cluster in each well was used to normalize the stimulated area per cluster. Table 1 summarizes the rock and fluid properties that were used in the current study.

Our analysis used the historic daily oil, gas, and water rates of the HFTS-1 wells and their associated P_{BH} for the first 3 years of production. Figure 5 shows an example of the three fluid rates for Well 3U. The gas-oil ratio (GOR) for the well started at around 800 scf/stb, then increased up

Fig. 3 Gunbarrel view of the HFTS-1 wells landed in the Upper and Middle WC analyzed in this study. Horizontal well spacing is 660 ft. Oblique distance between wells in the UWC and MWC various between 280 and 400 ft



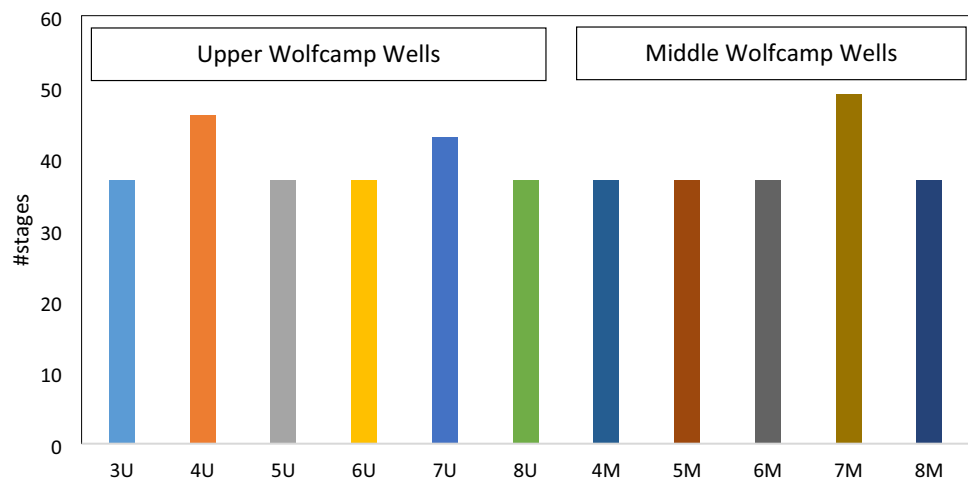
to 2000 scf/stb. High water production is associated with oil production in both production benches, for the UWC the water–oil ratio is about 1, and for the MWC it is about 2 (Weijermars et al. 2020). The RTA and GPT analyses were conducted on all of the 11 wells (see in Fig. 3) to

Table 1 Summary of the rock and fluid properties for the HFTS-1 wells

Reservoir temperature	156	F
Static reservoir pressure	4073	psi
Pressure (bubble point)	2350	psi
GOR	700	scf/stb
Oil compressibility	16.4E-06	psi ⁻¹
Average undersaturated oil compressibility	11.4E-06	psi ⁻¹
Oil	45.469	API
Gas gravity	0.7845	–
B _{ob}	1.4186	Bbl/stb
R _{sob}	779	Scf/stb

estimate the variations in the typical fracture half-length for each well in their stimulated reservoir regions.

Fig. 4 Number of stages for the Upper and Middle WC shale wells



Rate transient analysis

Figure 6 shows an example of the RTA analysis for Well 3U (one of the Upper WC wells). Figure 6a shows the diagnostic plot where the the pressure drop ($P_0 - P_{BH}$) is normalized using the production rate (water and oil combined, the gas flow was negligibly low). The normalized pressure difference and the derivative function were plotted against the material balance time (t_{mb}) in an RTA plot for flow regime diagnostics. The flow regimes can then be determined as a function of the tangent slopes to the plotted data. Figure 6a shows a linear flow regime with $\frac{1}{2}$ slope during most of the first year of production before it transitions to the boundary-dominated flow-regime with unit slope (Fig. 6a). This finding concurs with the flow regime analysis of Tugan and Weijermars (2022). The linear flow-regime region was further investigated with a square time plot to estimate the stimulated fracture area, according to Eq. (2) (Fig. 6b). The fracture half-length was normalized to be per stage, using the data of Fig. 4. Figure 6b was then used to estimate the slope m of the linear flow regime period. The value of $\sqrt{kA_c}$ was then estimated using Eq. (2). The formation and fluids properties were used based on the data on Table 1. In order to estimate the stimulated area, the formation permeability in the stimulated zone was assumed to be 100 nD. Nearby WC pilot wells gave GRI crushed sample permeability of

Fig. 5 Daily production rates for oil, gas, and water over the first 3-year production period for Well 3U

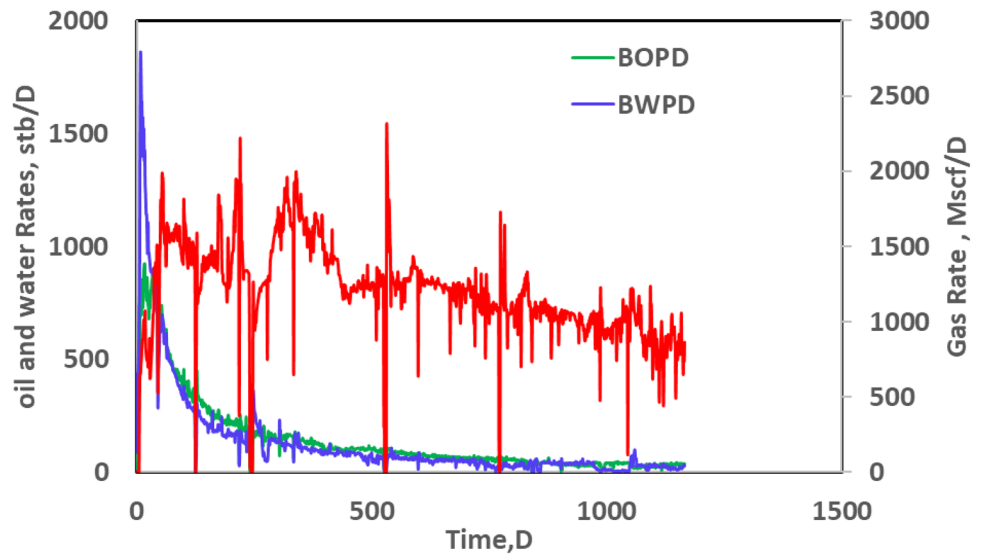


Fig. 6 RTA-plots for Well 3U. **a** Log/Log diagnostic plot $(P_0 - P_{BH})/q$, versus material balance time, and **b** RTA specialized plot for linear flow regime

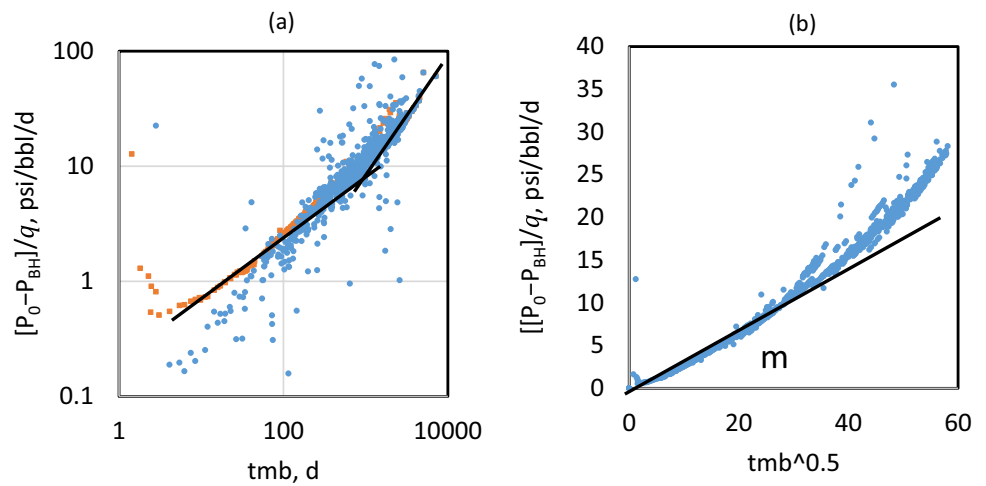


Table 2 Result for Upper Wolfcamp wells using RTA technique

Parameters	Unit	Well number					
		3U	4U	5U	6U	7U	8U
m	Psi/(bbl/d)/d ^{0.5}	0.21	0.29	0.22	0.24	0.24	0.30
$\sqrt{kA_c}$	ft ² .mD ^{0.5}	1.E5	1.3E5	9.7E4	9.1E4	9E4	7.1E4
k	nD	100	100	100	100	100	100
h_f	ft	100	100	100	100	100	100
n_f	Clusters	113	149	113	113	186	113
x_f	ft	229	222	217	203	122	158

300 nD (Pratama et al. 2023). However, we consider the GRI method overestimates the in-situ permeability, which we therefore downward adjusted to 100 nD.

In the present study, the average fracture half-length for each well was calculated using the following equation:

Table 3 Result for Middle Wolfcamp wells using RTA technique

Parameter	Unit	Well number				
		4M	5M	6M	7M	8M
m	Psi/(bbl/d)/d ^{0.5}	0.37	0.36	0.41	0.45	0.36
$\sqrt{k}A_c$	ft ² .mD ^{0.5}	8.1E4	8.5E4	7.3E4	7.2E4	8.3E4
k	nD	100	100	100	100	100
h_f	ft	100	100	100	100	100
n_f	Clusters	185	113	113	183	113
x_f	ft	108	184	156	95	175

$$A_c = 4n_f x_f h_f \quad (14)$$

where A_c is the stimulated area, n_f is the total number of fractures (which in this study was assumed equal to the total number of clusters), x_f is the fracture half-length, and h_f the fracture height in the pay zone (100 ft).

Tables 2 and 3 summarizes the RTA results for Upper and Middle WC wells. The total compressibility used in Eq. (2) was $5.10^{-5} \text{ psi}^{-1}$, which represents the total compressibility of the formation and the contained fluids. The linear flow regime slope was generally higher in the Middle WC wells as compared to the Upper WC wells. Hence, the stimulated area and fracture half-lengths estimated for the Middle WC wells were generally lower as compared to the Upper WC wells.

Gaussian pressure transient analysis

In the equivalent Gaussian RTA approach, the hydraulic diffusivity was first estimated from the production rates by history matching the actual well data. An example of the daily production data of Well 3U history-matched with Gaussian DCA (using Eq. (13)) is given in Fig. 7. The hydraulic diffusivity for all the HFTS-1 wells was constrained using Gaussian history matches, as was demonstrated in a prior study (Weijermars 2022b).

In a second step, the Gaussian forward model mode (using Eq. (12)) was applied to estimate the fracture half-lengths. A critical input is the permeability, which was in this study assumed to be 100 nD. This revises the results of the prior study which assumed a higher permeability of 500 nD (Weijermars 2022b) and a version of Eq. (13) with the porosity included resulting from an incorrect translation of Darcy velocity in the reservoir to Darcy flux from the reservoir into the wellbore. The resulting fracture-half lengths using the revised approach are summarized in Tables 4 and 5.

Discussion

Fracture half-length evaluation

Figure 8 summarizes the estimated fracture half-length for each of the 11 wells in the Upper and Middle WC that were part of the HFTS-1 projects. The average fracture half-length for the upper WC wells was found to be 184 ft and 171 ft, based on RTA and GPT analyses, respectively. These total averages indicate that the average deviation between the fracture half-lengths estimated by the two methods was 11%. The highest deviations were found for Wells 4U (20%), 7U (16%), and 3U (14%), and remained below 10% for the other three wells: 8U (8%), 6U (6%) and 5U (4%). At the base of the RTA method lies a constant well-rate solution of the diffusivity equation, while at the base of the GPT method lies a constant bottomhole solution for the same equation. Which of these two assumptions corresponds closer to reality will determine which estimation method is more realistic. Well 4U reached the constant bottomhole pressure condition later in the well life than the other wells hence the GPT and RTA estimation were slightly deviated from each other.

Likewise, the average fracture half-length for the Middle WC wells was found to be 144 ft and 136 ft, according to the RTA and GPT analyses, respectively. The average deviation between the two methods was found to be 10%. The maximum deviation occurred for Wells 7M (18%), 5M (12%), and 6M (11%), and remains below 10% for the Well 4M (8%) and 8M (3%). Our conclusion is that the two methods give comparable results, with GPT half-lengths on average about 10% shorter than obtained by the traditional RTA estimations. The deviation between the two methods for the data set used was 11% for the Upper WC wells and 10% for the Middle WC wells.

EUR impact of fracture half-length

The RTA and GPT results for each well were also compared against their oil and total fluid production. Higher fracture half-lengths indicate a higher stimulated area, which means for higher fracture lengths, higher oil and total fluid production volumes are expected. Figure 9 presents the cumulative

Fig. 7 Gaussian history matches HFTS-1 Well-3U using daily production (water and oil) data (blue dots) **a** Daily production. **b** Cumulative production, actual data in grey, and matches in red

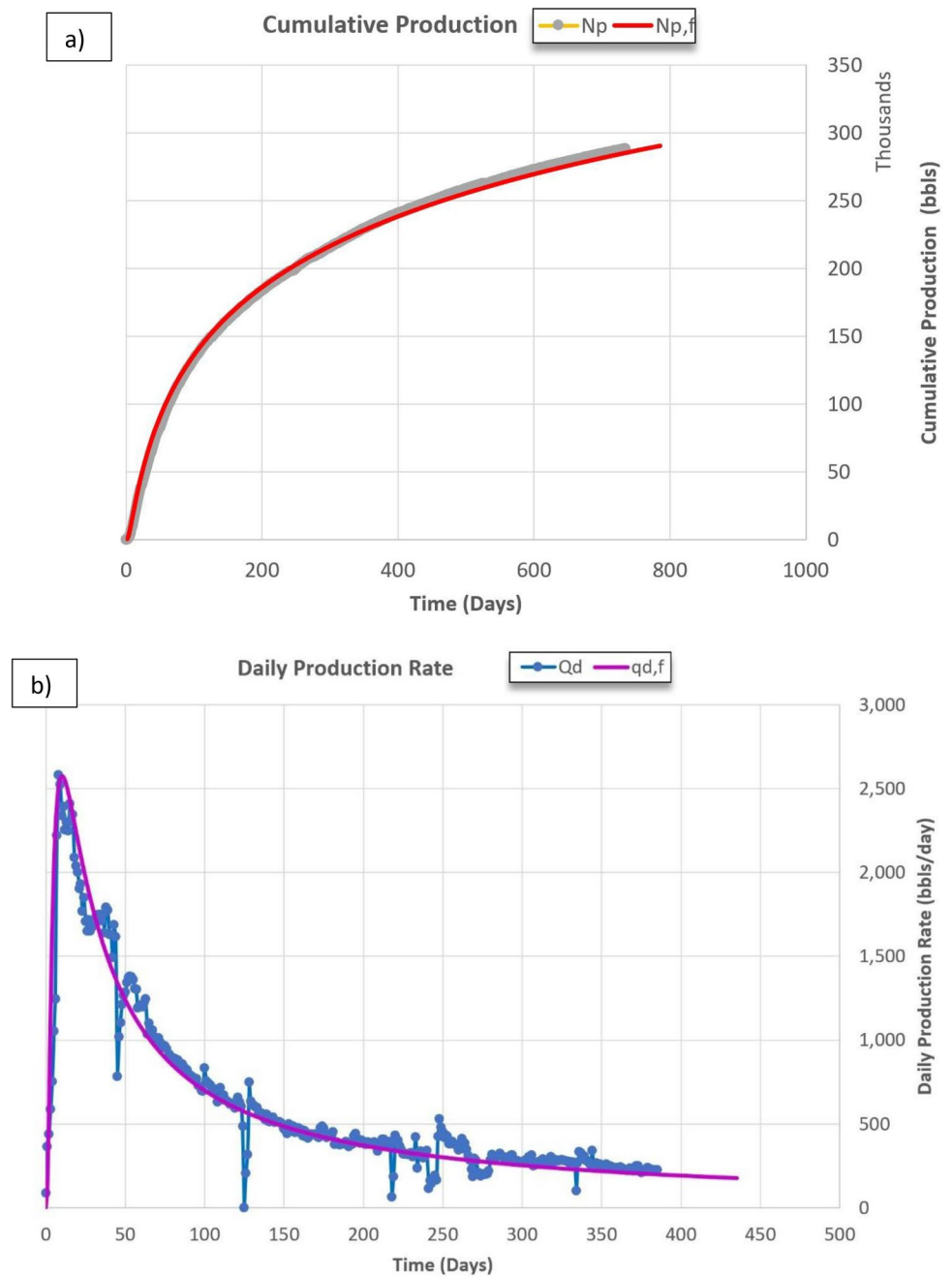


Table 4 Result for Upper Wolfcamp wells from GPT technique

Parameter	Unit	Well number					
		3U	4U	5U	6U	7U	8U
k	nD	100	100	100	100	100	100
D_h	ft ² /d	0.0222	0.0218	0.0220	0.0222	0.0223	0.0225
D_h	m ² /s	2.4E-8	2.3E-8	2.4E-8	2.4E-8	2.4E-8	2.4E-8
h_f	ft	100	100	100	100	100	100
n_f	Clusters	113	149	113	113	186	113
$2 x_f$	ft	394	286	416	380	282	292
x_f	ft	197	143	208	190	141	146

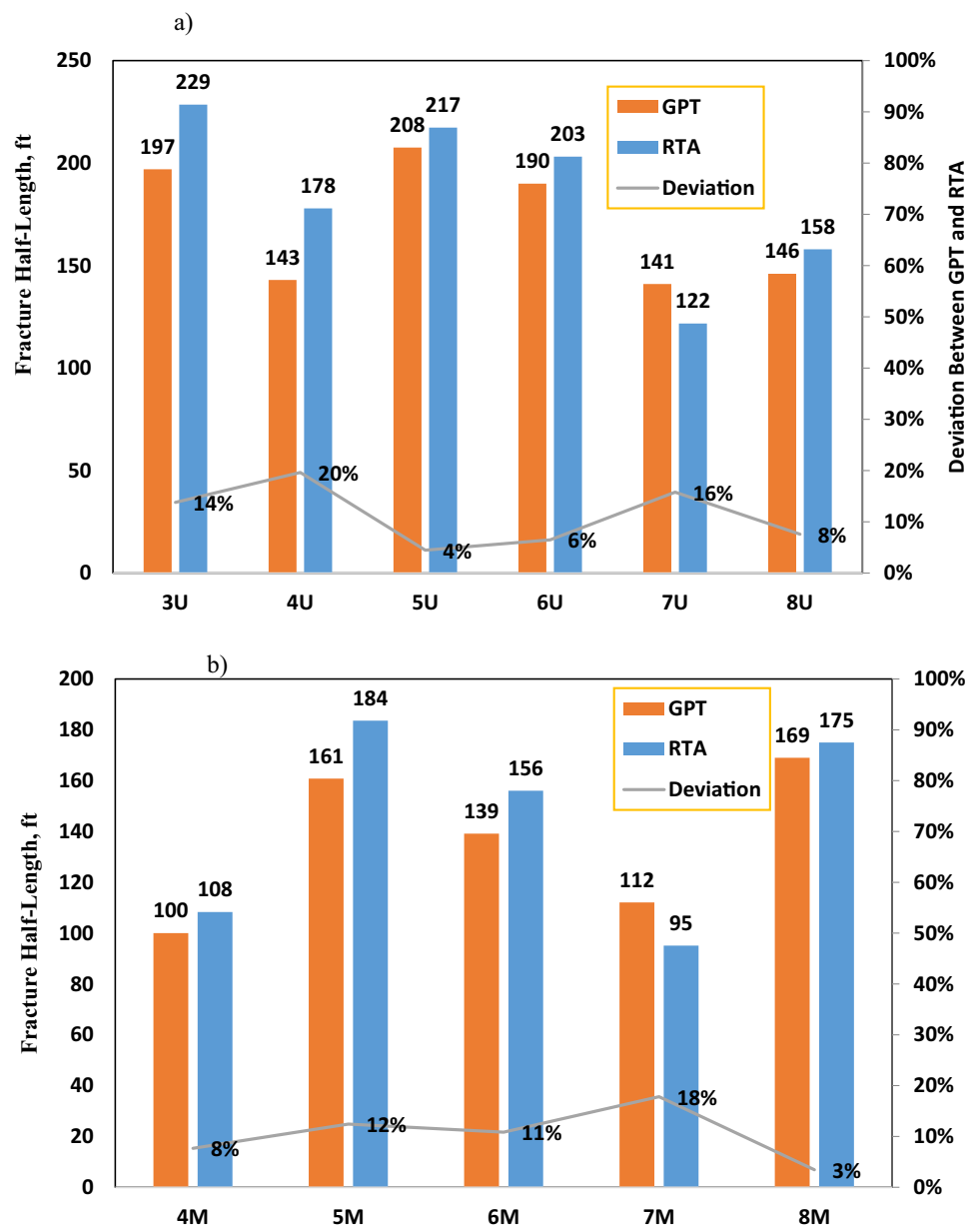
Table 5 Result for Middle Wolfcamp wells from GPT technique

Parameter	Unit	Well number				
		4 M	5 M	6 M	7 M	8 M
k	nD	100	100	100	100	100
D_h	ft ² /d	0.0225	0.0225	0.0228	0.0222	0.0224
D_h	m ² /s	2.4E-8	2.4E-8	2.5E-8	2.4E-8	2.4E-8
h_f	ft	100	100	100	100	100
n_f	Clusters	185	113	113	183	113
$2x_f$	ft	200	322	278	224	338
x_f	ft	100	161	139	112	169

oil and total fluid production after 3 years versus the estimated fracture half-length from RTA and GPT techniques. A linear relationship was found between x_f and the cumulative

production that confirms the reliability of GPT and RTA results. The Upper WC Formation wells (in red colors) showed higher production and stimulated area compared to

Fig. 8 Estimated fracture half-lengths for the HFTS-1 wells using the RTA and GPT-methods. **a** Upper WC wells (3U–8U), **b** Middle WC wells (4M–8M)



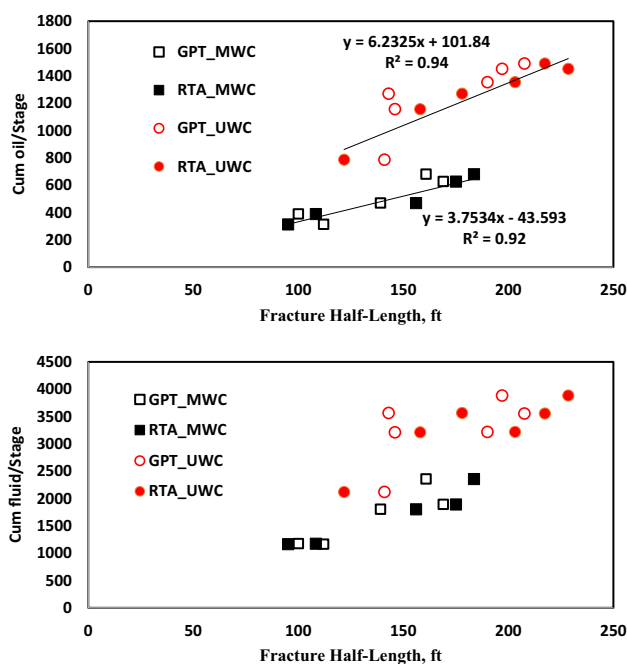


Fig. 9 Cumulative oil (a) and total fluid production (b) versus the fracture half-length from RTA and GPT-method for each of the 11 wells analyzed

Middle WC wells a possible reason for that is the higher proppant loading in Upper WC formation and lower water production. The EUR gain per ft fracture half-length is 6.2 bbl/ft for the Upper WC wells, and 3.7 bbl/ft for the Middle WC wells.

Proppant placement and fracture half-length

Figure 10 plots the fracture half-length versus the injected proppant volume, which reveals that with larger proppant injection volumes the fracture half-length increases, according to RTA and GPT estimations. Regression on the proppant load showed that increasing the proppant load leads to gains in fracture half-length of 3 ft/Mlb proppant load. Such fracture half-length increases benefit the EUR/well (Sect. "EUR impact of fracture half-length"). This is in agreement with the typical progress made in WC shale leases (Tugan and Weijermars 2022) and in the Eagle Ford shale play (Nandlal and Weijermars 2022). Previously, Srinivasan et al. (2018) presented how the evolution of the fracture design over years in all US shale basins showed increases in the proppant loading from around 500 lb/ft in the early times of 2011 to up to 2500 lb/ft in 2017 (Fig. 11); the average oil production increased from 40k bbls to 160K bbls, which reflects a better connection surface area between the wellbore and the formation through longer fracture half-lengths.

The results of the RTA and GPT approaches outlined here hinge on the accuracy of the data and the assumptions

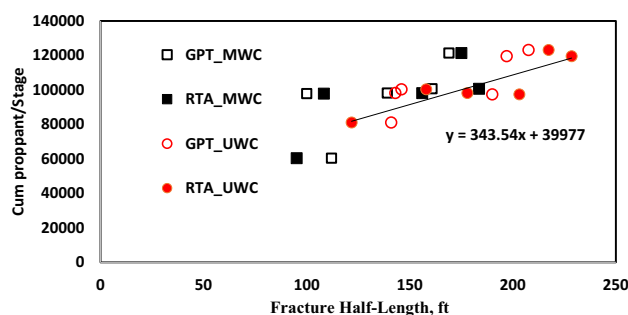


Fig. 10 Proppant load per stage versus fracture half-length, x_f

made. At the base of the RTA method lies a constant well-rate assumption to solve for the diffusivity equation, while at the base of the GPT method lies a constant bottomhole assumption to solve the same equation. Which of these two assumptions corresponds closer to reality will in part determine which of the two methods will yield the more realistic results. The present study uses deterministic inputs including specific values for the input parameters such as porosity, permeability, compressibilities, and formation thickness. Any uncertainty in these inputs may be reflected in the output in both methods that can be quantified through Monte Carlo sensitivity analysis. A study by Alvayed et al. (2023) performed sensitivity analyses using probability density functions and is complementary to the present study.

The assumption that the formation permeability in the stimulated zone is 100 nD has an important impact on the outcome of our results. The impact of the permeability on fracture half-length is given by \sqrt{k} in the RTA method (Eq. (6)), while it is linear in the GPT method (see Eq. (12)). In any case, the GRI crushed sample permeability of 300 nD (Pratama et al. 2023), is considered to overestimate the in-situ permeability. To examine the impact of the permeability in the estimated fracture half-length and the deviation between GPT and RTA, the fracture half-length was calculated using Eq. 6 and 12 at different permeabilities. Figure 12 presents the change in the fracture half-length as a function of assumed permeability. Both techniques showed similar behavior, with increasing the permeability the estimated half-length decreases. The deviation between the two methods was minimum at permeability of 64, however, the deviation slightly increased with increasing and decreasing the permeability to be up to 35% at permeability of 150 nd.

Conclusions

Hydraulic fracturing diagnostics is important for well planning and performance evaluation. Most diagnostic methods are syn-fracture and post-fracture, requiring the insertion of additional tools or injection of chemicals into the wells. The

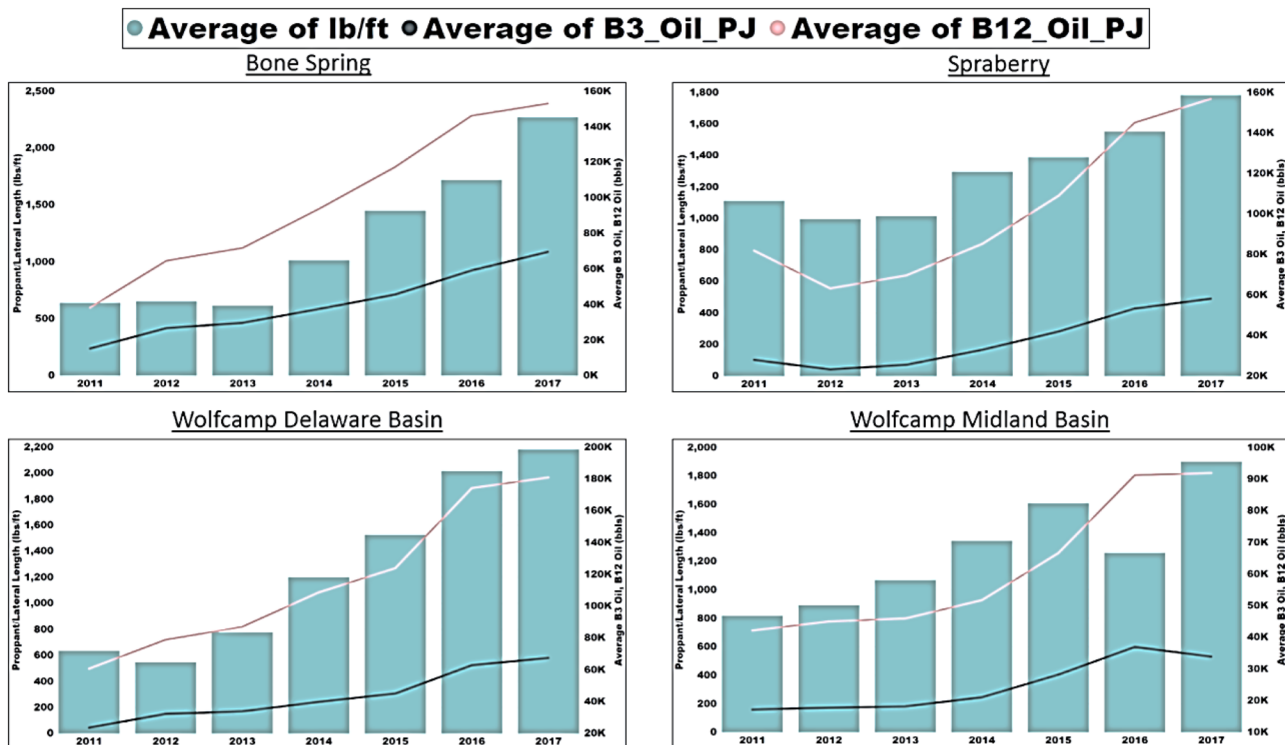


Fig. 11 Proppant loading, oil production over years for different basins, after Srinivasan et al. (2018)

current study presents the estimation of the fracture half-lengths with two different approaches. A recently developed Gaussian Pressure Transient (GPT) and the traditional rate transient analysis (RTA) techniques were used to evaluate different field production data for 6 wells in Upper Wolfcamp formation, and another 5 wells in Middle Wolfcamp formation. The following are the main findings.

- (1) Rate Transient Analysis and Gaussian Pressure Transient techniques yielded comparable fracture half-lengths with average deviation of 11% for the Upper Wolfcamp wells and 10% for the Middle Wolfcamp wells.
- (2) Rate Transient Analysis and Gaussian Pressure Transient techniques showed a linear relationship between the estimated fracture half-length and the cumulative

- production, which confirmed the mutual reliability of the GPT and RTA results.
- (3) The estimated ultimate recovery (EUR) gain per fracture half-length is 6.2 bbl/ft for the Upper Wolfcamp wells, and 3.7 bbl/ft for the Middle Wolfcamp wells.
- (4) Regression on the proppant load showed that increasing the proppant load leads to gains in fracture half-length of 3 ft/Mlb proppant load.

The findings show the capabilities of RTA and GPT for fracture diagnostics that contribute to improved well planning, performance evaluation, and optimization of fracture stimulation treatments.

Funding The authors of this article would like to acknowledge the support provided by King Fahd University of Petroleum & Minerals (KFUPM) to publish this work.

Declarations

Conflict of interest The authors declare that they have no known competing financial interests or personal relationships that could have appeared to influence the work reported in this paper. The authors declare that there is no external fund for this study. The authors would like to thank KFUPM for giving permission to publish this work.

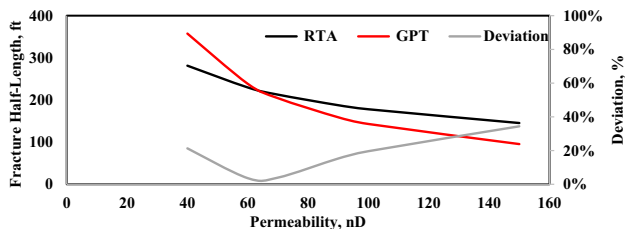


Fig. 12 Impact of assumed permeability on the estimated fracture half-length from GPT and RTA methods

Open Access This article is licensed under a Creative Commons Attribution 4.0 International License, which permits use, sharing, adaptation, distribution and reproduction in any medium or format, as long as you give appropriate credit to the original author(s) and the source, provide a link to the Creative Commons licence, and indicate if changes were made. The images or other third party material in this article are included in the article's Creative Commons licence, unless indicated otherwise in a credit line to the material. If material is not included in the article's Creative Commons licence and your intended use is not permitted by statutory regulation or exceeds the permitted use, you will need to obtain permission directly from the copyright holder. To view a copy of this licence, visit <http://creativecommons.org/licenses/by/4.0/>.

References

- Al-Fatlawi O, Hossain M, Patel N et al (2019a) Evaluation of the potentials for adapting the multistage hydraulic fracturing technology in tight carbonate reservoir. In: Proceeding paper presented at the SPE middle east oil and gas show and conference, Manama, Bahrain, March 2019a. Paper number: SPE-194733-MS. <https://doi.org/10.2118/194733-MS>
- Al-Fatlawi O, Hossain M, Essa A (2019b) Optimization of fracture parameters for hydraulic fractured horizontal well in a heterogeneous tight reservoir: an equivalent homogeneous modelling approach. Paper presented at the SPE Kuwait oil & gas show and conference, October 13–16. Paper number: SPE-198185-MS. DOI: <https://doi.org/10.2118/198185-MS>
- Alipour M, Esatyana E, Sakhaee-Pour A et al (2021) Characterizing fracture toughness using machine learning. *J Petrol Sci Eng* 200:108202
- Alipour K, Mehdi K, Sakhaee-Pour A et al (2022) Empirical relation for capillary pressure in shale. *Petrophysics* 63(05):591–603
- Alvayed D, Khalid MSA, Dafaalla M, Ali A, Ibrahim AF, Weijermars R (2023) Probabilistic estimation of hydraulic fracture half-lengths: validating the Gaussian pressure-transient method with the traditional rate transient analysis-method (Wolfcamp case study). *J Petrol Explor Prod Technol* 1–16
- Barree RD, Fisher MK, & Woodroof RA (2002) A practical guide to hydraulic fracture diagnostic technologies. Paper presented at the SPE annual technical conference and exhibition, San Antonio, Texas, September 2002. Paper number: SPE-77442-MS. <https://doi.org/10.2118/77442-MS>
- Clarkson CR (2013) Production data analysis of unconventional gas wells: review of theory and best practices. *Int J Coal Geol* 109:101–146. <https://doi.org/10.1016/j.coal.2013.01.002>
- Ciezobka J, Courtier J, and Wicker J (2018) Hydraulic fracturing test site (HFTS)-project overview and summary of results. In: Proceeding paper presented at the SPE/AAPG/SEG unconventional resources technology conference, Houston, Texas, USA, July 2018. Paper Number: URTEC-2937168-MS. <https://doi.org/10.15530/URTEC-2018-2937168>
- Cipolla CL, Williams MJ, Weng X, Mack M, & Maxwell S (2010, December) Hydraulic fracture monitoring to reservoir simulation: maximizing value. Paper presented at the SPE annual technical conference and exhibition, Florence, Italy, September 2010. Paper number: SPE-133877-MS. <https://doi.org/10.2118/133877-MS>
- Dheyauldeen A, Alkhafaji H, Alfarge D, Al-Fatlawi O, Hossain M (2022) Performance evaluation of analytical methods in linear flow data for hydraulically-fractured gas wells. *J Petrol Sci Eng* 208:109467
- E1-Banbi AH, & Wattenbarger RA (1998) Analysis of linear flow in gas well production. SPE Gas technology symposium, Calgary, Alberta, Canada, March 1998. Paper number: SPE-39972-MS, pp 1–18. <https://doi.org/10.2118/39972-MS>
- Esatyana E, Sakhaee-Pour A, Sadooni FN, Al-Kuwari HAS (2020) Nanoindentation of shale cuttings and its application to core measurements. *Petrophysics* 61(05):404–416
- Fujian Z, Hang S, Liang X et al (2019) Integrated hydraulic fracturing techniques to enhance oil recovery from tight rocks. *Pet Explor Dev* 46(5):1065–1072
- Holditch SA (2010) Hydraulic fracturing and well completion. In: Thaxton K, Arthur D, Langhus B (eds) *Modern fracturing—enhancing natural gas production*. ET Publishing, Virginia Gardens
- Ibrahim M, & Wattenbarger RA (2005) Analysis of rate dependence in transient linear flow in tight gas wells. In: Canadian international petroleum conference 2005, CIPC 2005, Calgary, Alberta. Paper number: PETSOC-2005–057. <https://doi.org/10.2118/2005-057>
- Ibrahim AF, Nasr-El-Din HA, Rabie A, Lin G, Zhou J, Qu Q (2018) A new friction-reducing agent for slickwater-fracturing treatments. *SPE Prod Oper* 33(03):583–595. <https://doi.org/10.2118/180245-PA>
- Ibrahim AF, Assem A, Ibrahim M (2020) A novel workflow for water flowback RTA analysis to rank the shale quality and estimate fracture geometry. *J Nat Gas Sci Eng* 81:103387
- Ibrahim M, Wattenbarger RA (2006) Rate dependence of transient linear flow in tight gas wells. *J Canad Petrol Technol* 45(10). <https://doi.org/10.2118/06-10-TN2>
- King GE (2012) Hydraulic fracturing 101: What every representative, environmentalist, regulator, reporter, investor, university researcher, neighbor and engineer should know about estimating frac risk and improving frac performance in unconventional gas and oil wells. In: Proceeding paper presented at the SPE hydraulic fracturing technology conference, The Woodlands, Texas, USA, February 2012. Paper Number: SPE-152596-MS. <https://doi.org/10.2118/152596-MS>
- Lee J, Rollins JB, Spivey JP (2003) *Pressure transient testing*. Society of Petroleum Engineers, Texas
- Li W, Sakhaee-Pour A (2016) Macroscale Young's moduli of shale based on nanoindentations. *Petrophysics* 57(06):597–603
- Maxwell SC, Rutledge J, Jones R, Fehler M (2010) Petroleum reservoir characterization using downhole microseismic monitoring. *Geophysics* 75(5):75A129-75A137
- Murillo GG, Rodriguez JA, Centeno JS, Medina E, & Perez A (2014, May) Application of concepts to improve oil production in low-permeability turbidite reservoirs in Mexico. Paper presented at the SPE Latin America and Caribbean Petroleum Engineering Conference, Maracaibo, Venezuela, May 2014. Paper Number: SPE-169263-MS. <https://doi.org/10.2118/169263-MS>
- Nandlal K, Weijermars R (2022) Shale well factory model reviewed: eagle ford case study. *J Petrol Sci Eng* 212:110158. <https://doi.org/10.1016/j.petrol.2022.110158>
- Nashawi IS, & Malallah A (2006) Rate derivative analysis of Oil Wells intercepted by finite conductivity hydraulic fracture. In: Canadian International Petroleum Conference, Calgary, Alberta, June 2006. Paper Number: PETSOC-2006–121. <https://doi.org/10.2118/2006-121>
- Nguyen KH, Zhang M, Ayala LF (2020) Transient pressure behavior for unconventional gas wells with finite-conductivity fractures. *Fuel* 266:117119
- Nobakht M, Clarkson CR, Kaviani D (2012) New and improved methods for performing rate-transient analysis of shale gas reservoirs. *SPE Reserv Eval Eng* 15(03):335–350
- Pakhotina I, Sakaida S, Zhu D, Hill AD (2020) Diagnosing multistage fracture treatments with distributed fiber-optic sensors. *SPE Prod Oper* 35(04):0852–0864
- Peebles A, Al-muntasheri G, Sullivan R (2018) Successful production of oil and gas from shales with nano-Darcy range permeability: selecting a nano-scale proppant. Presented at the SPE/AAPG eastern regional meeting, October 7–11, 2018. Paper

- Number: SPE-191826–18ERM-MS. DOI: <https://doi.org/10.2118/191826-18ERM-MS>
- Pratama MA, Al-Qoroni O, Rahmatullah IK, Jameel MF, & Weijermars R (2023) Probabilistic production forecasting and reserves estimation: benchmarking Gaussian against the traditional arps decline curve analysis method (Wolfcamp Shale Case Study). *Geoenergy Science and Engineering*, in revision
- Sakaïda S, Pakhotina I, Zhu D, & Hill AD (2022, January) Estimation of fracture properties by combining DAS and DTS measurements. Paper presented at the SPE international hydraulic fracturing technology conference & exhibition, January 11–13, 2022. Paper Number: SPE-205233-MS. DOI: <https://doi.org/10.2118/205233-MS>
- Sakhaee-Pour A, Bryant SL (2012) Gas permeability of shale. *SPE Reserv Eval Eng* 15(04):401–409
- Sakhaee-Pour A, Li W (2019) Two-scale geomechanics of shale. *SPE Reserv Eval Eng* 22(01):161–172
- Shabani M, Ghanizadeh A, Clarkson CR (2022) Permeability measurements using rate-transient analysis (RTA): comparison with different experimental approaches. *Fuel* 308:122010
- Smith MB, Montgomery C (2015) *Hydraulic fracturing*. CRC Press
- Srinivasan K, Ajisafe F, Alimahomed F, Panjaitan M, Makarychev-Mikhailov S, & Mackay B (2018, September) Is there anything called too much proppant?. Paper presented at the SPE Liquids-Rich Basins conference—North America, September 5–6, 2018. Paper Number: SPE-191800-MS. DOI: <https://doi.org/10.2118/191800-MS>
- Tian W, Wu X, Shen T, Kalra S (2016a) Estimation of hydraulic fracture volume utilizing partitioning chemical tracer in shale gas formation. *J Nat Gas Sci Eng* 33:1069–1077
- Tian W, Shen T, Liu J et al (2016b). Hydraulic fracture diagnosis using partitioning tracer in shale gas reservoir. Paper presented at the SPE Asia Pacific hydraulic fracturing conference, Beijing, China, August 2016b. Paper Number: SPE-181857-MS. <https://doi.org/10.2118/181857-MS>
- Tran H, Sakhaee-Pour A (2017) Viscosity of shale gas. *Fuel* 191:87–96
- Tran H, Sakhaee-Pour A (2018a) Slippage in shale based on acyclic pore model. *Int J Heat Mass Transf* 126:761–772
- Tran H, Sakhaee-Pour A (2018b) Critical properties (T_c , P_c) of shale gas at the core scale. *Int J Heat Mass Transf* 127:579–588
- Tran H, Sakhaee-Pour A (2019) The compressibility factor (Z) of shale gas at the core scale. *Petrophysics* 60(04):494–506
- Tugan MF, Weijermars R (2022) Searching for the root cause of shale well-rate variance: highly variable fracture treatment response. *J Petrol Sci Eng* 210:109919. <https://doi.org/10.1016/j.petrol.2021.109919>
- Warpinski NR, Mayerhofer MJ, Vincent MC, Cipolla CL, Lolon EP (2009) Stimulating unconventional reservoirs: maximizing network growth while optimizing fracture conductivity. *J Can Pet Technol* 48(10):39–51
- Weijermars R (2021) Diffusive mass transfer and Gaussian pressure transient solutions for porous media. *MDPI Fluids* 6(11):379. <https://doi.org/10.3390/fluids6110379>
- Weijermars R (2022a) Production rate of multi-fractured wells modeled with Gaussian pressure transients. *J Petrol Sci Eng* 210:110027. <https://doi.org/10.1016/j.petrol.2021.110027>
- Weijermars R (2022b) Gaussian decline curve analysis method: a fast tool for analyzing hydraulically fractured wells in shale plays demonstrated with examples from HFTS-1 (hydraulic fracture test site-1, Midland Basin, West Texas). *MDPI Energies* 15(17):6433. <https://doi.org/10.3390/en15176433>
- Weijermars R, Afagwu C (2022) Hydraulic diffusivity estimations for US shale gas reservoirs with Gaussian method: implications for pore-scale diffusion processes in underground repositories. *J Nat Gas Sci Eng*. <https://doi.org/10.1016/j.jngse.2022.104682>
- Weijermars R, Nandlal K, Tugan MF, Dusterhoft R, & Stegent N (2020) Hydraulic fracture test site drained rock volume and recovery factors visualized by scaled complex analysis models: emulating multiple data sources (production rates, Water Cuts, Pressure Gauges, Flow Regime Changes, and b -sigmoids). Paper presented at the SPE/AAPG/SEG unconventional resources technology conference, Virtual, July 2020. Paper Number: URTEC-2020–2434-MS. <https://doi.org/10.15530/urtec-2020-2434>
- Wattenbarger RA, El-Banbi AH, Villegas ME, Maggard JB (1998) April. Production analysis of linear flow into fractured tight gas wells. Paper presented at the SPE Rocky Mountain Regional/Low-Permeability Reservoirs Symposium, Denver, Colorado, April 1998. Paper Number: SPE-39931-MS. <https://doi.org/10.2118/39931-MS>.

Publisher's Note Springer Nature remains neutral with regard to jurisdictional claims in published maps and institutional affiliations.